identification of unknown biomolecules in tissue samples. Thus the high mass resolution of the FT-ICR-MS can be used to analyze compounds that cannot be distinguished with lower–mass resolution mass spectrometers (Taban *et al.*, 2007; Wang *et al.*, 2011). MALDI-FT-ICR has also been reported for IMS analysis of drugs and metabolites in tissue. The accurate mass measurement can be performed using FT-ICR-MS, which provided a molecular specificity for the ion images obtained from tissue sample analysis (Cornett *et al.*, 2008).

5. IMS MEASUREMENTS

MALDI-IMS experiments can be performed after the deposition of matrix on the tissue section and using different types of MS instruments as discussed above. The setting of the laser energy, detector gain, and random walk function are optimized in order to obtain better signal intensity of the target molecules during the IMS analysis. Either a particular region of the tissue or the entire tissue section is selected for analysis, depending on the particular interest. At present, the commercially available instruments can perform IMS analyses with the highest spatial resolution of $\sim 25\,\mu m$ (Goto-Inoue *et al.*, 2009a). Recently we developed a mass microscope that can move a sample stage by $1\,\mu m$, and the finest size of the laser diameter is approximately $10\,\mu m$ (Harada *et al.*, 2009). The measurement time of IMS experiments depends on the number data spots, the frequency of the laser, and the number of shots per spot.

6. DATA ANALYSIS

Due to the large (gigabytes) size of the dataset, high-capacity visualization software is required to visualize the ion image and distribution pattern of biomolecules in tissue samples. New computing methods are required for both rapid, accurate data acquisition and the interpretation of the IMS analysis results. Therefore, in addition to instrumental improvements, data acquisition and software development have been important for the production of reliable data. The databases used are based on algorithms that perform analysis through statistical evaluation of observed and theoretical spectra of bimolecules. BioMap (http://www.maldi-msi.org, Novartis, Basel, Switzerland) and flexImaging (http://www.bdal.com, Bruker Daltonics GmbH, Bremen, Germany) imaging software are used to identify biomolecules in various sample types. The intensity of the different color images obtained by both software packages can relate the distribution of biomolecules in the tissue section. These software packages also help in understanding the localization of biomolecules at

particular regions of interest (ROIs) for mass spectral comparison and other statistical analysis.

BioMap imaging software can be used for different instruments such as PET, nuclear magnetic resonance (NMR), computed tomography (CT), and near-infrared fluorescence (NIRF) as the result of multiple modifications. Interactive data language Virtual Machine (Research Systems, Boulder, CO) is required in the system to process the data obtained from IMS analysis. BioMap software can also be used for baseline correction, spatial filtering, and averaging of spectra for presentation of the IMS results.

The flexImaging software is used for the acquisition and evaluation of MALDI-TOF imaging results. The mass peaks (at m/z) obtained in the mass spectrum are normalized to total ion current and then the peak intensity is taken into account to study the molecules distribution on the tissue section. The imaging MS experiments are performed by collecting spectra at a resolution of 50 to 400 μm in the same m/z range as above. Principal component analysis (PCA) is an unsupervised statistical method used to identify groups of closely correlated variables; for MS imaging datasets these variables are spatial coordinates and mass. This approach also reduces the multidimensional datasets to the lower dimensions (Chou, 1975). PCA analysis is performed using ClinProTools 2.1 software (Bruker Daltonics). Zaima *et al.* (2009) performed a PCA for screening of metabolites in the fatty liver. Several differences were found in identifying the metabolites in fatty and normal liver tissue samples. PCA was also used in proteomics studies (Deininger *et al.*, 2008; Djidja *et al.*, 2010; Yao *et al.*, 2008).

7. APPLICATIONS OF IMS FOR DIRECT ANALYSIS OF TISSUE

7.1. IMS for Lipidomics

Lipids are the main constituents of cell membranes; the major functions of lipids are transportation of ions and signals across the cell membrane. Various types of lipids, such as glycerophospholipids (GPLs), sphingolipids, sterol lipids, saccharolipids, waxes, and fat-soluble vitamins are found in biological systems. Membranes act as barriers to separate compartments within eukaryotic cells and to separate all cells from their surroundings (Brown, 2007; Fahy *et al.*, 2009; Lee *et al.*, 2003). The identification and quantification of lipids in tissue sample can help in understanding several biosynthetic and metabolic pathways that govern human diseases, such as insulin-resistant diabetes, Alzheimer's disease, schizophrenia, cancer, atherosclerosis, and infectious diseases (Oresic *et al.*, 2008). Thus the analysis of lipids in tissue samples is a very important issue. High-performance liquid chromatography (HPLC) (McCluer *et al.*, 1986), TLC (Touchstone,

1995), and MS have been used to analyze lipids in tissue samples. However, the sample preparation procedures in chromatographic techniques are lengthy and the localization of biomolecules in tissue sample surface cannot be established. Therefore, different IMS systems are successfully used for imaging of lipids. The analysis of glycerophospholipids, sphingolipids, and neutral lipids is discussed in detail in the following sections.

7.1.1. Glycerophospholipids

GPLs are glycerol-based phospholipids and essential components of cell membranes. They act as second messengers involved in cell proliferation, apoptosis, and metabolism. The determination of GPL content in tissue samples is useful for finding potential biomarkers for diseases such as atherosclerosis or rheumatism (Fuchs *et al.*, 2005; Schmitz and Ruebsaamen, 2010). Altered levels of lipids are found in many pathological conditions such as Alzheimer's disease (Han *et al.*, 2001, 2002), Down syndrome (Murphy *et al.*, 2000), diabetes (Han *et al.*, 2007), and Niemann–Pick disease (He *et al.*, 2002). Figure 10 illustrates the basic structures of common classes of GPLs such as PC, phosphatidylethanolamine (PE), phosphatidylinositol (PI), and phosphatidylserine (PS) (Jackson and Woods, 2009). PC is easily ionized due to its charged quaternary ammonium head group and has thus become a popular lipid species to investigate (Pulfer and Murphy, 2003). The ionized molecules observed in the mass spectrum are usually either protonated $[M+H]^+$, sodiated $[M+Na]^+$, or pottasiated $[M+K]^+$ in positive-ion mode. Phospholipids such as PE, PS, PA, PG, and PI may generate negative ions due to the presence of the phosphodiester moiety and display molecular anions $[M-H]^-$ (Fuchs *et al.*, 2010). The addition of potassium acetate (Sugiura *et al.*, 2009) or LiCl (Jackson *et al.*,

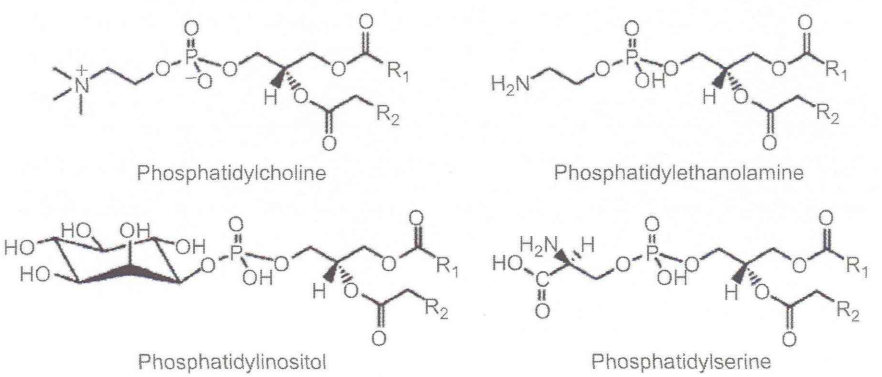

FIGURE 10 Structure of glycerophospholipids. Reprinted from Jackson and Woods (2009) with permission from Elsevier Science.

2005) to the matrix solution has also been reported for effective ionization of molecules in tissue samples.

The selection of MALDI matrices is an important issue. For MALDI-IMS, the matrix should have good vacuum stability and homogenous crystal formation containing analyte molecules. Various matrices have been reported for the identification and characterization of lipids in MALDI-MS, including DHB (Petkovic *et al.*, 2001; Puolitaival *et al.*, 2008; Schiller *et al.*, 1999), DHA (Jackson *et al.*, 2005; Shimma *et al.*, 2007), p-nitroaniline (PNA) (Estrada and Yappert, 2004; Rujoi *et al.*, 2004), and 9-aminoacridine (Eibisch and Schiller, 2011; Teuber *et al.*, 2010). However, PNA and dihydroxyacetone phosphate (DHAP) were unstable under high vacuum conditions and started to evaporate after their introduction into the MALDI-MS instrument (Jackson *et al.*, 2005; Rujoi *et al.*, 2004; Shrivas *et al.*, 2010). DHB matrix exhibited a lower sensitivity for the detection of PA, PS, PE, PI, and PG in negative-ion mode, possibly due to its acidity (Estrada and Yappert, 2004; Petkovic *et al.*, 2001). DHA can be used in both positive and negative ionization modes for analysis of phospholipids (Woods *et al.*, 2006). PNA is another good matrix for the analysis of phospholipids in either positive-ion or negative-ion modes (Estrada and Yappert, 2004). Recently, 2-mercaptobenzothiazole (MCT) was added as an alternative to the use of DHB for MALDI-MS analysis of phospholipids in brain and liver tissue samples (Astigarraga *et al.*, 2008). The main advantages of MCT over the commonly used matrices DHB, DHA. and PNA are low vapor pressure, low acidity, and homogenous crystal formation, which allowed for detection of more lipid species in negative mode, with high sensitivity and high detection reproducibility. Ionic matrices have also been used in MALDI-IMS owing to the good vacuum stability, homogenous crystal formation, and good solubility of analytes for efficient ionization and desorption of molecules (Chana *et al.*, 2009; Lemaire *et al.*, 2006a; Shrivas *et al.*, 2010). Shrivas *et al.* (2010) used an ionic matrix of CHCAB to image and identify lipids in mouse cerebellum and found that this ionic matrix yields a higher number of ion images compared with the use of DHB matrix in MALDI-IMS (Figure 11). Use of NPs is another good approach for selective and sensitive analysis of lipids and small metabolites in tissue samples without matrix-oriented peaks in the low-molecular-mass range (Cha and Yeung, 2007; Goto-Inoue *et al.*, 2010a; Hayasaka *et al.*, 2010; Shrivas *et al.*, 2011; Taira *et al.*, 2008).

Sugiura *et al.* (2009) showed the imaging of polyunsaturated fatty acid–containing PC in mouse brain using MALDI-IMS. The results demonstrated that arachidonic acid (AA) and DHA-containing PC were found in the hippocampal neurons and cerebellar Purkinje cells, respectively. Figure 12 shows the localization of PC species in different layers of the mouse brain (Sugiura *et al.*, 2009). The distribution of PC species also has been reported in the mouse retinal section via MALDI-IMS analysis. The localization of PC (16:0/18:1) was found in the inner nuclear layer and

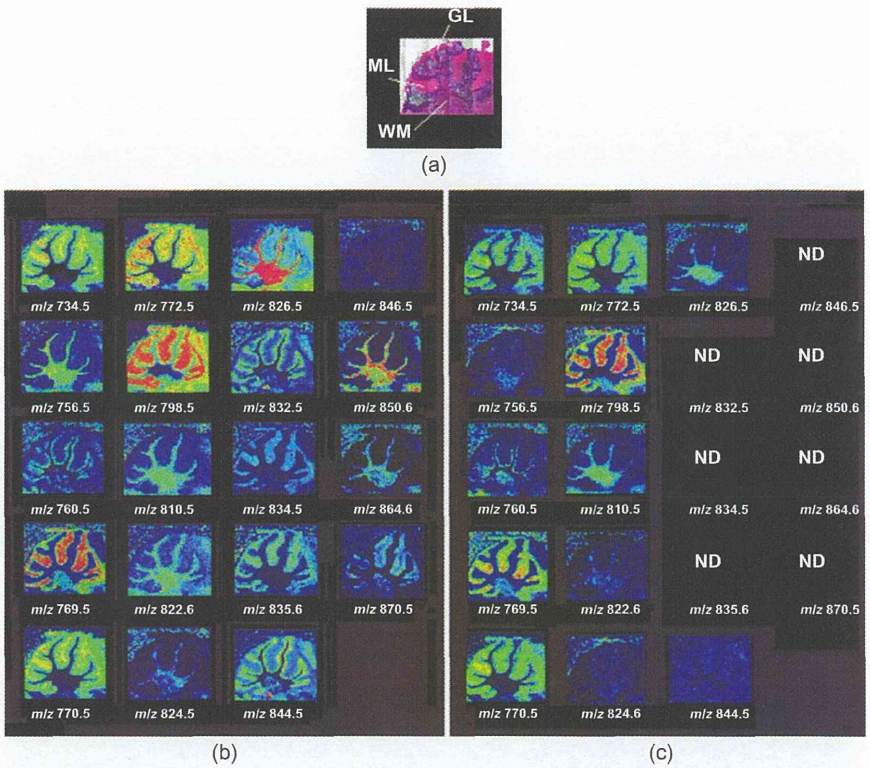

FIGURE 11 (a) H&E-stained mouse cerebellum showing three layers with 1.5-mm scale bar (white color). The ion images of lipids in mouse cerebellum tissue section obtained by using (b) CHCAB and (c) DHB as a matrix at m/z 734.5 $[(PC(16:0/16:0)+H)]^+$, 770.5 $[PC(16:0/16:1)+K]^+$, 772.5 $[PC(16:0/16:0)+K]^+$, 798.5 $[PC(16:0/18:1)+K]^+$, 834.5 $[PC(18:0/22:6)+H]^+$, and 870.5 $[PC(18:1/22:6)+K]^+$ were localized in the molecular layer of cerebellum; at m/z 760.5 $[PC(16:0/18:1)+H]^+$, 832.5 $[PC(18:0/20:4)+Na]^+$, 844.5 $[PC(16:0/22:6)+K]^+$, and 846.5 $[PC(18:1/20:4)+K]^+$ were specific to the granular layer; and at m/z 756.50 $[PC(16:0/16:0)+Na]^+$, 810.5 $[PC(18:0/18:1)+Na]^+$, 824.5 $[PC(18:0/18:2)+K]^+$, and 826.5 $[PC(18:0/18:1)+K]^+$ and were found to be concentrated in the white matter of cerebellum. The ion images *at* m/z 769.5 $[SM(d18:1/18:0)+K]^+$ and 835.6 $[SM(d18:1/24:1)+Na]^+$ illustrated that the molecules were distributed in the region of molecular layer of tissue. The ion images at m/z822.6 $[GalCer(d18:1/22:0)+K]^+$ and 850.6 $GalCer(d18:1/24:0)+K]^+$ were localized in the white matter of mouse cerebellum. ND indicates the molecules were not detected. GL, granular layer; ML, molecular layer; WM, white matter. Reprinted from Shrivas *et al.* (2010) with permission from American Chemical Society.

the outer plexiform layer; PC (16:0/16:0) in the outer nuclear layer and inner segment; and PC (16:0/22:6) and PC (18:0/22:6) in the outer segment and pigment epithelium (Hayasaka *et al.*, 2008). Differential localization of PC (16:0/20:4) species was observed between terminal and stem villi of

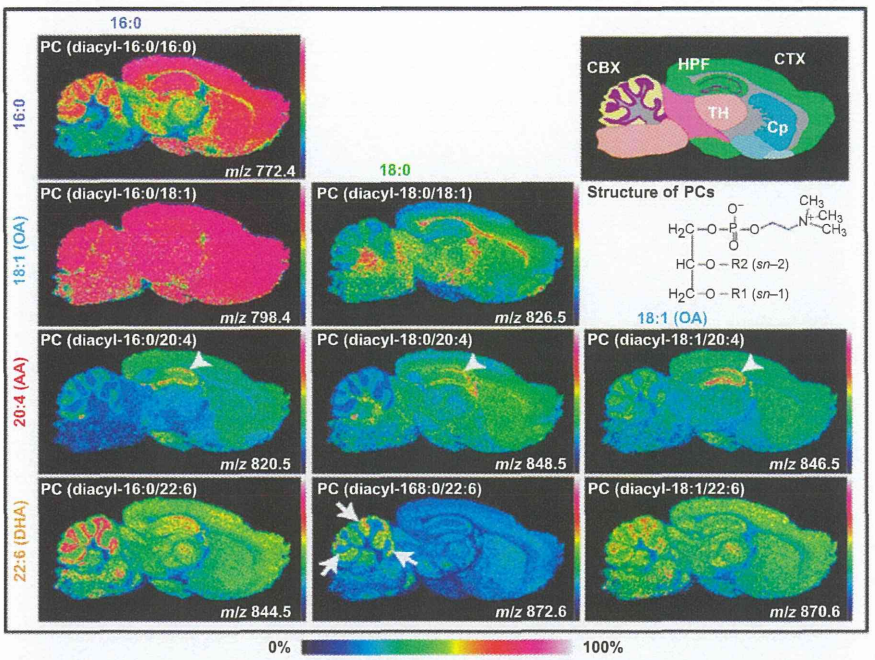

FIGURE 12 Identification of molecular species of PC in sagittal mouse brain sections by MALDI-IMS. Among the PC, AA-PC showed characteristic localization in the hippocampal cell layers (arrowheads). Among DHA-containing species, two abundant species, PC (diacyl-16:0/22:6) and PC (diacyl-18:1/22:6), were commonly enriched in the granule layer of the cerebellum, while PC (diacyl-18:0/22:6) showed a characteristic dotted distribution pattern near the cell layer (arrows). CBX, cerebellar cortex; CP, corpus striatum; CTX, cerebral cortex; HPF, hippocampal formation; TH, thalamus. Reprinted from Sugiura *et al.* (2009) with permission from the American Society for Biochemistry and Molecular Biology.

human placenta, which could be helpful in understanding the pathological involvement of fetal growth restriction and fetal hypoxia (Kobayashi *et al.*, 2010). The accumulation of lipid molecules, such as LPC (1-acyl 16:0), PC (1-acyl 36:4), and shingomyelin (SM) (d18:1/16:0) around the damaged valvular region was investigated and suggested an association of these molecules with tissue inflammation and resultant valvular incompetence (Tanaka *et al.*, 2010). PC (diacyl-16:0/20:4) containing an AA was found at higher concentration in prefrontal cortex tissue compared with occipital cortex tissue in the brains of patients with schizophrenia (Matsumoto *et al.*, 2011). The specific localization of five PC species in the cochlea was also examined using the mass microscope. A differential distribution of PC species was observed; (16:0/18:1) in the organ of Corti and the stria vascularis, (16:0/18:2) in the spiral ligament, and (16:0/16:1) in the organ of Corti (Takizawa *et al.*, 2010). Recently Goto-Inoue *et al.* (2009a)

investigated use of a TLC-Blot-MALDI-IMS for analysis and characterization of acidic, neutral glycosphingolipids and PC in sample mixtures. In TLC-Blot, the lipids are separated and transferred to a polyvinylidene fluoride (PVDF) membrane without any change in the stability of the molecules. PVDF membranes with the sample may then be placed on the target plate for MALDI-IMS analysis. This method might be useful for the detection of minor components that could not be detected by the conventional TLC method. SIMS is also used for imaging of lipids at high spatial resolution and sensitive detection. The combined approaches of MALDI-IMS and SIMS-IMS have been used for imaging of PC in cultured mammalian neuron. The data obtained from MALDI and SIMS supported that the signals of small molecules in the low molecular region, such as PC head groups and fatty acids (detected in SIMS) were obtained from the intact lipids (Yang *et al.*, 2010). DESI-IMS has been used for imaging of most commonly encountered brain lipid species such as PE and PI in rat spinal cord cross sections in negative-ion mode. The ion image of PI (38:4) was shown in grey matter regions such as the cortex and hippocampus. The ion image of PE (at m/z 888) showed the white specific region in the brain (Dill *et al.*, 2009).

7.1.2. Sphingolipids

The sphingolipid is a type of lipid obtained from the aliphatic amino alcohol sphingosine. The main functions of sphingolipids are transmission and cell recognition. The investigation of sphingolipids is very important because they are indicative of aging and may function as a disease marker. Sphingolipids contain a sphingoid base backbone and include sphingomyelins (SM), sulfatides (ST), ceramides, cerebrosides, and gangliosides (Merrill *et al.*, 2009) (Figure 13). Changes in the levels of lipids,

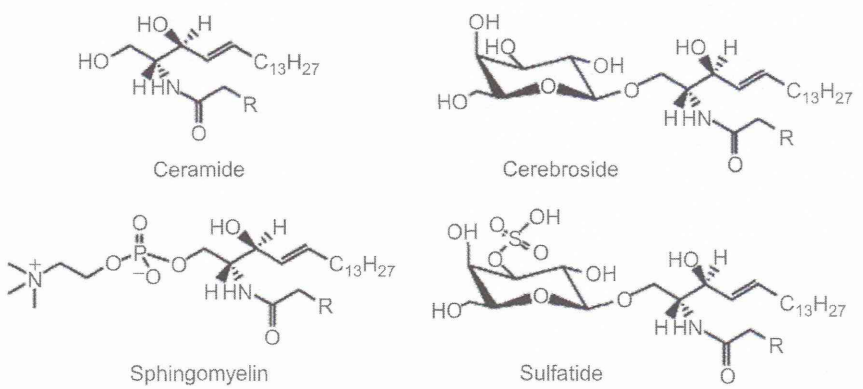

FIGURE 13 Structure of sphingolipids. Reprinted from Jackson and Woods (2009) with permission from Elsevier Science.

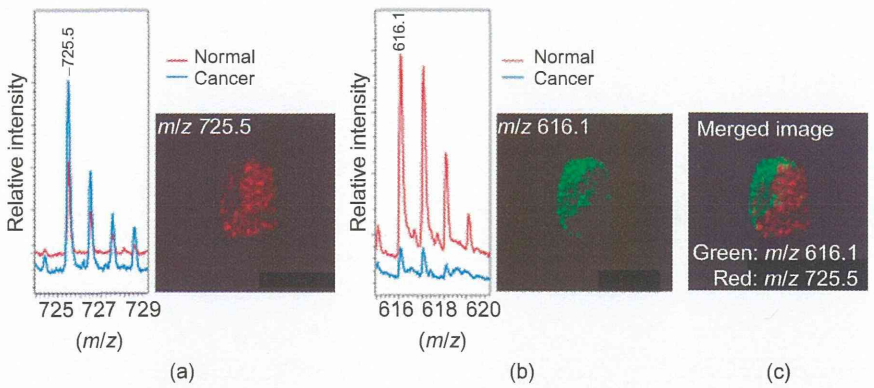

FIGURE 14 Imaging of normal and cancerous cells in human liver sample. (a) The most prominent signal at m/z 725 showed the higher expression for cancerous cells than normal cells. (b) The signal at m/z 616 showed the higher distribution of this molecule in normal cells. (c) Merged images at m/z 725 and 616. Reprinted from Shimma *et al.* (2007) with permission from Elsevier Science.

in particular ceramide, also have been observed in apoptosis or cell death (Fuchs *et al.*, 2007; Thomas *et al.*, 1999). MALDI-MS/MS analyses were used to image liver tissue samples at a thickness 3 μm from a patient with colon cancer. A higher expression of sphingomyelin (SM, 16:0) at m/z 725 was observed in cancerous tissue than in normal tissue by MS/MS analyses (Figure 14). In contrast, a strong distribution of an ion at m/z 616 was observed in the normal but not cancerous tissue sample (Shimma *et al.*, 2007). IMS has also been used to detect seminolipid, a glycolipid synthesized in sperm. Here, seminolipid localization was performed in mice testis during testicular maturation Goto-Inoue *et al.* (2009b). In another study, the distribution pattern of ganglioside molecular species (C-18 and C-20) in mouse hippocampus was demonstrated using MALDI-IMS. The localization of C-18 species was found in the frontal brain and C-20 species contained in the entorhinal-hippocampus projections of the molecular layer (ML) of the dentate gyrus. Figure 15 shows the distribution of C-20-sphingosine–containing gangliosides in the hippocampal formation (Sugiura *et al.*, 2008). In a study using gold NPs in Nano-PALDI-IMS and comparing it with the use of DHB matrix, the PI, ST, and ganglioside species (GM3, GM2, GM1, GD1, and GD3) were all detected with higher sensitivity. This is the first report of the visualization of minor sphingolipids by IMS analyses using gold NPs in tissue sections (Goto-Inoue *et al.*, 2010). Higher expression of sulphatides in ovarian cancer cells was reported compared with a normal sample with MALDI-IMS analysis and similar results were obtained by a transcriptomic approach of lipid analysis (Liu *et al.*, 2010). The high spatial resolution localization of glucosylceramide in spleen of a mouse model of Gaucher disease was

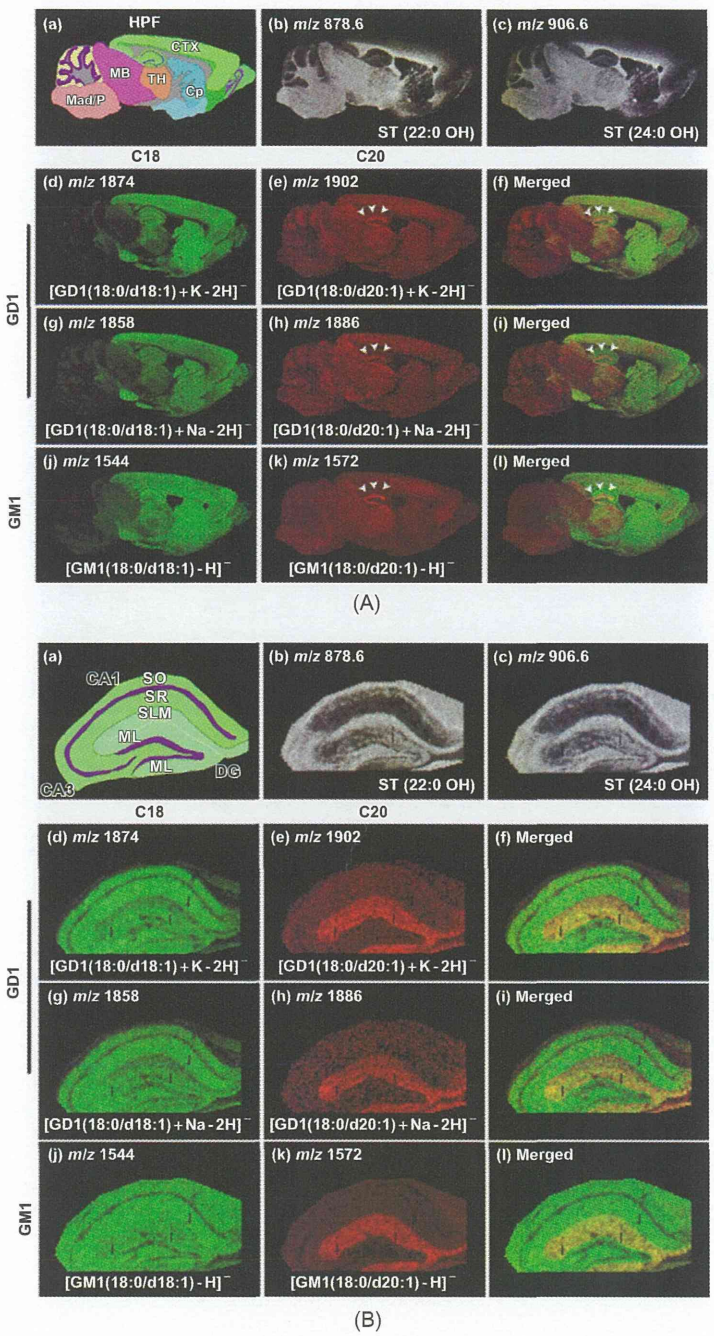

FIGURE 15 (Continued)

FIGURE 15 Localization of C20-sphingosine–containing gangliosides in the hippocampal formation. IMS at 50-mm raster step size was used to gain an overview of ganglioside distribution in different brain regions (A), and IMS at 15-mm raster size was used to study in detail the distribution pattern of gangliosides in the hippocampus (B). In both panels, schematic diagram of the brain section (a) and ion images of STs (b)–(c) are presented. For ions corresponding to the GD1 molecular species, we observed the ion distributions of both sodium and potassium complexes; that is, the ions at m/z 1858 (f) and m/z 1886 (g), which correspond to the $[M+Na-H]^-$ form of C18- and C20-GD1, and those at m/z 1874 (h) and m/z 1902 (i), which correspond to the $[M+K-H]^-$ form of C18- and C20-GD1, respectively. The ion distribution patterns corresponding to the GD1-Na salts and GD1-K salts are fairly uniform for both C18- and C20-species. For GM1, m/z 1544 (d) and m/z 1572 (e), which correspond to C18- and C20-sphingosines–containing GM1, respectively, are shown. HPF, hippocampus formation; MadP, ————————-; CTX, cerebral cortex; MB, ————————-; TH, Thalamus; SO,————————-; SR, stratum radiatum; SLM, stratum lacunosum molecular; ML, molecular layer. Reprinted from Sugiura *et al.* (2008) with permission from Public Library of Science.

also demonstrated using MALDI-IMS (Snel and Fuller, 2010). Ganglioside GM2, asialo-GM2 (GA2), and sulfatides in brain from a mouse model of Tay-Sachs/Sandhoff disease (Chen *et al.*, 2008) and sulfatides in mouse kidney (Marsching *et al.*, 2011) have been reported.

7.1.3. Nonpolar Lipids

Imaging and identification of nonpolar lipid in tissue sections is not easy, perhaps because of the difficulty in the ionization of molecules in MALDI-MS. Thus only a few species of nonpolar lipids have been successfully reported. One example is cholesterol, a highly abundant lipid in many tissues. It is usually detected at m/z 369 after the loss of a water molecule using an organic matrix in MALDI-MS. Cholesterol is a vital constituent of the cell membrane, required for lipid organization and cell signaling. Changes in the quantity of cholesterol in tissue can cause myocardial infarctions and stroke, as well as other disorders (Fernandez *et al.*, 2011). SIMS has been used for imaging of cholesterol with the capability to analyze single cells. In this setup one drawback was that cholesterol was fragmenting (Piehowski *et al.*, 2008). However, the use of NIMS could directly analyze the brain cholesterol metabolites in Smith-Lemli-Opitz syndrome without the fragmentation of molecules in MS (Patti *et al.*, 2010). The distribution of triglycerides (TAG) in mouse embryo was also investigated using MALDI-IMS (Hayasaka *et al.*, 2009). TAG is an ester derived from glycerol and three fatty acids and is the main constituent of vegetable oil and animal fats. Figure 16 is illustrates the distribution of different molecular species of TAG $[(16:0/18:2/18:1)+Na]^+$, $[(16:0/18:1/18:1)+Na]^+$, $[(16:0/20:3/18:1)+K]^+$ in mouse embryo. The ion images of TAG were concentrated mainly around the brown adipose and liver tissue (Hayasaka *et al.*, 2009).